



SACRED HEART RESEARCH PUBLICATIONS

Journal of Functional Materials and Biomolecules

Journal homepage: www.shcpub.edu.in



ISSN: 2456-9429

Optical studies on Dysprosium doped copper oxide nanoparticles synthesized by combustion technique

John.D.Rodney¹, S. Deepapriya¹, P. Annie Vinosha¹, S. Krishnan², M. Cyril Robinson³, S. Jerome Das^{1*}

Received on 18 May 2019, accepted on 7 June 2019

Published online on 12 June 2019

Abstract

Metal Oxides have adaptable applications in the arena of nanomaterials because of their inimitable applicable properties. Amidst these metals oxides, copper oxide nanoparticles are well recognized because of their narrow bandgap and multivariate physic-chemical properties. Undoped and 3% dysprosium doped copper oxide nanoparticles were synthesized using combustion technique which is inexpensive and time effective unlike other synthesis techniques. The content of fuel/oxide ratio in this method concludes and restricts the nature of the nanoparticles synthesized. Structural and optical characterizations of the processed nanoparticles were implemented using X-ray diffractometer, UV-Vis spectrometer, Fourier transform infrared spectrometer, transmission electron microscope and Raman spectrometer. The crystallite size, nature and monoclinic structure of CuO were revealed and confirmed from the XRD pattern. And UV-Vis spectrum broadcasts the materials optical properties and the band gap was confirmed using the Kubalka-Munk plot. The FTIR spectra showcased the different vibrational modes present in the system. The microstructural nature of the as-prepared particles was determined using Raman spectrum. The individualized morphological inquisition and the size of the CuO nanoparticles were determined by TEM.

Keywords: combustion technique; copper oxide; Dysprosium; Optical properties

1 Introduction

For the bygone few periods, the study of metal oxide semiconductor nanoparticles became a major field of research, Due to their explanatory physic-chemical properties[1]. Among any other transitional metal oxides, Copper Oxide has fascinated a massive range of people because of its various properties which are effectively suitable for formulating a diversity of efficient equipment's and systems. It is drawing researchers vowing to be a

promising material due to its abundance in nature; cost effective and non-toxic nature[2]. The p-type monoclinic structured copper oxide comes under a wide range of transitional metal oxide. It is known for exhibiting versatile optical, catalytic and electrical properties. It is also acknowledged for its breathtaking impact in the field of batteries, sensors, capacitors, solar cells etc.,[3] etc. The CuO nanoparticles show an array of adaptation on structural and optical properties when doping element is added. These modifications in the properties are in reliance upon the form and concentration of doping element. As in the case of doping material, R.E. elements are generally chosen due to its exemplar characteristic of confining the grain boundaries and thus in turn altering the nature and property of the material Further, R.E doped materials improves the optical and electrical conductivity of host oxides. Metal oxide nanoparticles can be synthesized by numerous chemical methods like the sol-gel [3], solution combustion [4], co-precipitation [5], spray pyrolysis [6], solvothermal [7] etc. Out of which the combustion synthesis was considered due to its cost and time effective parameter in the preparation of nanoparticles. In this routine of fabricating metal oxides, the materials used in fuel/oxidizer and the oxidizer-fuel ratio [8] make a decision over the properties of synthesized particles. In this assessment we have doped trivalent Dy³⁺ ions into copper oxide nanoparticles and the structural, morphological and optical activities were investigated and reported.

2 Experimental

2.1 Chemicals:

All chemicals (copper (II) nitrate tri-hydrate Cu(NO₃)₂·3H₂O, glycine C₂H₅NO₂ and dysprosium (III) nitrate hex-ahydrate Dy H₁₂N₃O₁₅) in high purity were acquired from Merck and used without any additional refinement for the synthesis of Dy doped CuO nanoparticles.

* Corresponding author: e-mail jeromedas.s@gmail.com; jerome@loyolacollege.edu

^{1,*}Department of Physics, Loyola College, Chennai – 600 034, India.

²Department of Physics, Ramakrishna Mission Vivekananda College, Chennai-600 004, India

³Department of Physics, Madras Christian College, Chennai – 600 059, India

2.2 Synthesis of 3% Dy doped copper oxide Nanoparticles:

3%Dy doped CuO nanoparticles was prepared by solution combustion method. Primarily the solution was prepared by dissolving the Oxidizer-Fuel materials[9], Copper nitrate trihydrate, dysprosium (III) nitrate hexahydrate and glycine were added in 100 ml of distilled water with an appropriate stoichiometric ratio. The O/F ratio of redox mixture was sustained to unity[10]. The solution is further agitated at constant rpm for 1hour in a glass beaker using magnetic stirrer to obtain a homogenous mixture. The solution was then heated using a mantle and when the ignition temperature reaches, the mixture gets auto-ignited and with rapid evolution of gas in large volume results in fine powder. The resultant powder was ground well and characterized for various properties.

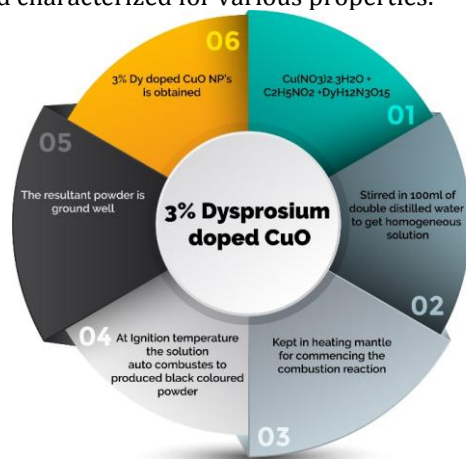


Fig.1 A schematic illustration of the synthesis procedure of 3% Dy doped CuO NP's.

3 Results and Discussion

3.1 Structural Analysis: X-Ray Diffraction

The typical XRD pattern for pure and 3% dysprosium doped copper oxide nanoparticles is as shown in fig.2. The most protruding peaks were noted down and was cross verified with JCPDS card number 89-5895[9]. It is seen that no Cu_2O residue peaks were found, thus retaining the monoclinic structure of CuO rather than cubic.

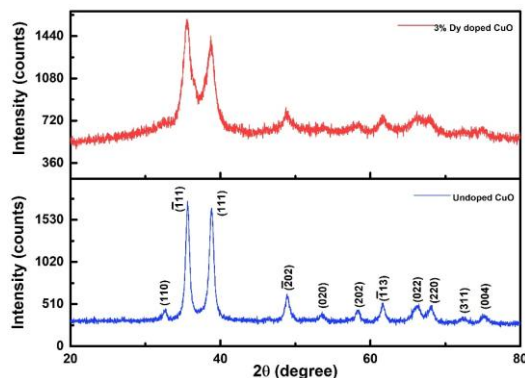


Fig.2 XRD Pattern of undoped and 3% Dy doped CuO nanoparticles

It is imbedded from the spectra, as the Dy^{3+} ions are added to the system, it is possible that the Dy^{3+} ions are assimilated on to the matrix of CuO forming Dy-Cu-O. As

the dopant is added, there is a slight reduction in the intensity of the peak and anupsurge in the peak width when compared with the Pure CuO pattern. This action is formly due to the incorporation of Dy^{3+} ions on to the CuO crystal lattice. The variation in the ionic radii of the host and dopant leads to a stress and strain factor induced into the system leading to the reduction in the crystallite size. The Scherrer's formula was used to decipate the average crystallite size.[11](Eq. (1))

$$D = \frac{0.9\lambda}{\beta \cos \theta} \quad (1)$$

Where β is is Full Width at Half Maximum (FWHM) of the peaks at the diffracting angles θ and λ is the wavelength of X-ray radiation[12].Using convoluting Gaussian profile the β can be found from FWHM. The broadening β_r is,

$$\beta_r^2 = \beta_0^2 - \beta_i^2 \quad (2)$$

Where β_i is the instrumental broadening and β_0 is observed broadening. The average crystallite size and change in lattice parameters are listed down in table.1.

Table.1 lattice parameters and crystallite size of undoped and 3% Dydoped CuO nanoparticles

sample	a (Å)	b (Å)	c (Å)	D (nm)
Pure CuO	4.7158	3.4146	5.0702	13.5
3% Dy doped CuO	4.5065	3.4211	5.1862	6.2

From the table we recognize that the lattice parameters a, b, c are not equal to each other and as the dopant is added there is a slight shift in peak width vowing to a much smaller crystallite size and deviation in the lattice parameters. This adjustment in parameters is due to the doping of Dy^{3+} ions, for they have a tendency to confine the grain boundaries restricting the growth of the particle thus leaving to a much reduced crystallite size.

3.2 FTIR Analysis

The vibrational modes and functional groups present in as-synthesized material was characterized by Perkin-Elmer spectrum FT-IR spectroscopy for a range of 4000-450 cm^{-1} at room temperature[13]. Fig. 3 exhibits the FTIR spectra of pure and 3% Dy doped CuO. In general, the vibration bands of Metal-Oxygen bonds are observed below 600 cm^{-1} . The peaks at 509 and 510 cm^{-1} for pure CuO and 3% Dy doped CuO respectively, were assigned to vibration of Cu-O bond. The wide transmittance band at 3851, 3427, 1386 cm^{-1} and 3428, 1384 cm^{-1} of pure and 3% Dy doped CuO correspondingly were formed due to O-H bond vibrations[14], these peaks exemplifies the moisture absorbing property of material. The minute vibrational peak at 2353 cm^{-1} represents the O=C=O bond[15], which was present as residue from the synthesis technique. The shift in the transmittance bands indicates that there is a complexion of CuO and dysprosium.

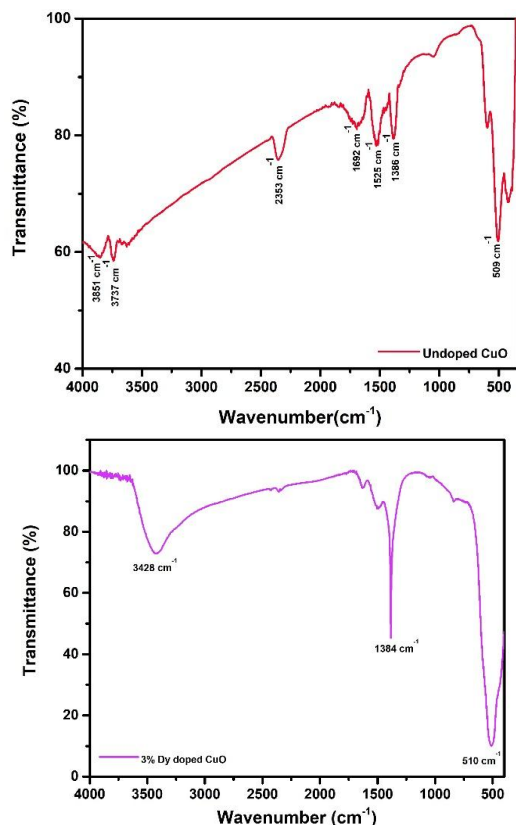


Fig. 3 FTIR spectra of pure and 3% Dy doped CuO

3.3 Morphological Analysis: TEM

Fig.4 showcases the morphology of as-grown pure CuO and 3% Dy doped CuO nanoparticles investigated by TEM. It is significant to note that only uniform growth of spherical particles were attained from the whole sample and no other shape was obtained[16]. As the dopant is added, there is a decline in the particle size, which in-turn increases the surface to volume ratio. The pressure induced effect and the grain boundary confining property of the dopant over the host leads to aabridged particle size.

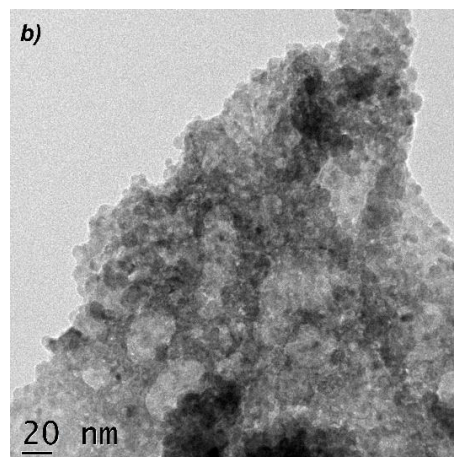
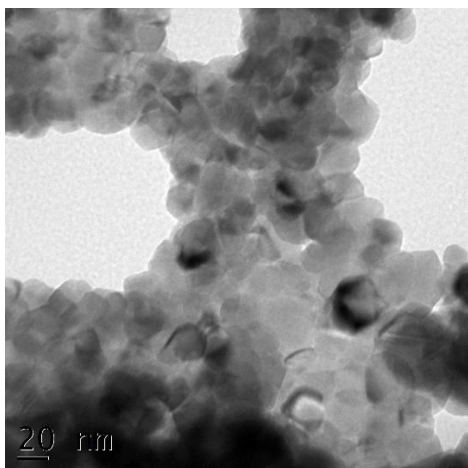


Fig. 4 TEM micrograph of a) pure and b) 3% Dy doped CuO

3.4 Optical Analysis: UV-Vis

The optical analysis of the synthesized pure and 3% Dy doped CuO was undertaken using Agilent Carey 5000 UV Visible spectrophotometer for a range of 200 to 700 nm[17]. From fig.5 the absorption band of pure and 3% Dy doped CuO a nanoparticle was found to be widely inside the visible region.

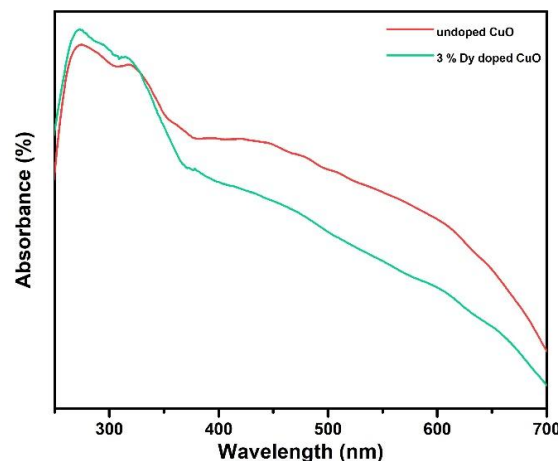


Fig. 5 Absorbance band of Pure and 3% Dy doped CuO

Where as fig.6 showcases the energy structure of the as-prepared nanoparticles. The absorption coefficient is used to define the optical energy gap E_g using the Kubulka-Munk plot and the equation is as follows[18]:

$$(\alpha h\nu) = C(\alpha h\nu - E_g)^2 \quad (3)$$

Where, E_g is the optical bandgap energy, C is the constant for direct transition and α is the absorption coefficient. The bandgap energies of the undoped and 3% Dy doped CuO is determined by inferring a linear portion of $(\alpha h\nu)^2$ onto energy axis where α is zero.

The band gap energy of undoped and 3% Dy doped CuO was noted to be 1.95 and 1.85 eV respectively. Due to weak quantum confinement effect, the undoped nanoparticles exhibited higher bandgap when compared with bulk confirming a blue shift when reduced to nanoscale [19]. In comparison with pure sample, the Dy doped samples shows a gradual red shift in optical absorption region. This slender movement can be

endorsed to the depiction of the Dy³⁺ ions on the host material. As the surface pressure in the particle increases due to the reduced size, the lattice strain also increases which diminutions the bandgap.

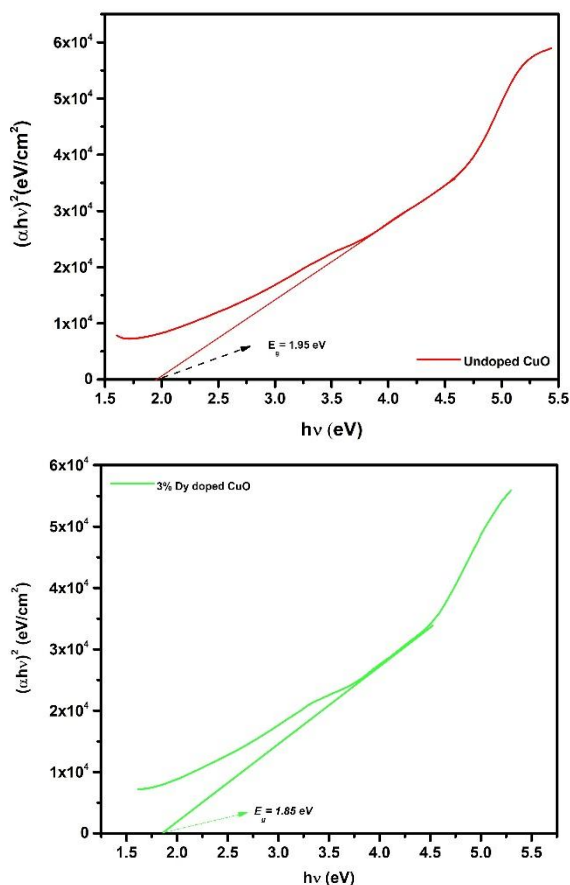


Fig. 6 Kubelka-Munk plot for Pure and 3% Dy doped CuO

3.5 Optical Analysis: Raman

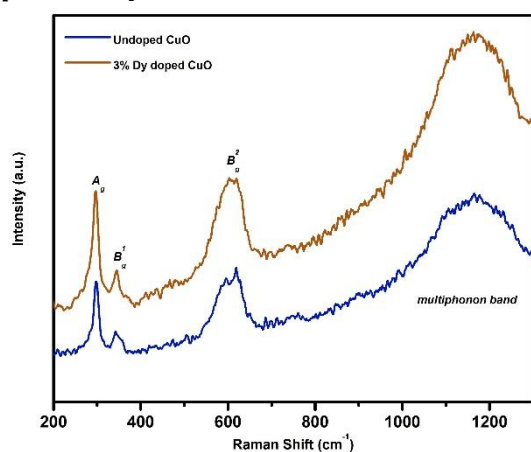


Fig. 7 Raman Spectra of Pure and 3% Dy doped CuO

The Raman spectra of pure and 3% Dy doped CuO NP's is as shown in fig. 7. The copper oxide NP's are primarily a part of the C_{6h} space group and the intricate portrayal associated with the lattice vibrations of a primitive cell is given as [20]

$$\Gamma_{RA} = 4A_u + 5B_u + A_g + 2B_g \quad (14)$$

Overall group theory predicts 3 raman active modes (A_g+2B_g), 6 infrared modes and 3 acoustic modes out of 12 modes of vibrations. It is well seen that the three raman active modes were present determining the CuO electronic transitions and the vibration of oxygen atoms. As the dopant is added an increase in its intensity was seen and no unpremeditated phases like the Cu₂O were visible. This increase in the intensity of the peaks can be attributed to the smaller size of the given material and the slight red shift is endorsed to the phonon confinement effect of the nano materials. Apart from these three active raman vibrational modes, a multiphonon band [21] was noted around 1160 cm⁻¹ for both undoped and doped material with varied intensities. The formation of the band is hugely contributed to the electronic density variation which leads to the stretching vibration in the x²-y² plane and is related to the phonon-phonon inharmonic coupling in polar solids.

4 Conclusions

In summary, pure and 3% Dy doped copper oxide has been successfully synthesized via solution combustion technique using an appropriate oxidizer-fuel proportion. The as-synthesized particles were subjected to XRD, FT-IR, UV-Visible, TEM and RAMAN to realize their structural, optical and morphological properties. From XRD analysis, the monoclinic structure was identified and it is seen that the crystallite sizes were reduced as dysprosium is doped. The shift and variation in the XRD spectrum manifested the presence of dysprosium in CuO which resulted in reduction of lattice parameters. And from the FTIR spectrum, the metal oxide peak confirms the existence of CuO vibrational mode. UV- visible absorption spectrum intimates the existence of slight red shift in band gap. Due to smaller size, the lattice strain gets increased which tune downs the band gap from 1.95 to 1.85 eV and the Raman spectra confirms the presence of all the three raman modes with also a manifestation of a multi phonon band.

References

- [1] Zhang Q, Zhang K, Xu D, Yang G, Huang H, Nie F, Liu C and Yang S 2014 CuO nanostructures: Synthesis, characterization, growth mechanisms, fundamental properties, and applications *Prog. Mater. Sci.* **60** 208-37
- [2] Hwang H, Lee K Y, Yeo T and Choi W 2015 Investigation of structural and chemical transitions in copper oxide microstructures produced by combustion waves in a mixture of CuO-Cu₂O-Cu and fuel *Appl. Surf. Sci.* **359** 931-8
- [3] Abdul Rahman I B, Ayob M T M, Mohamed F, Othman N K, Mohd Lawi R L and Radiman S 2012 Synthesis and Characterization of ZnO, CuO and CuO/ZnO Nanostructures by a Novel Sol-Gel Route under Ultrasonic Conditions *Adv. Mater. Res.* **545** 64-70

- [4] Mukasyan A S, Rogachev A S and Aruna S T 2015 Combustion synthesis in nanostructured reactive systems *Adv. Powder Technol.***26**
- [5] Vinosha P A, Mely L A, Mary G I N, Mahalakshmi K, Vinosha P A, Mely L A, Mary G I N, Mahalakshmi K and Das S J 2017 Study on Cobalt Ferrite Nanoparticles Synthesized by Co-Precipitation Technique for Photo-Fenton Application *Meachanics, Mater. Sci. Eng.* 1-6
- [6] Vijayalakshmi S, Venkataraj S, Subramanian M and Jayavel R 2008 Physical properties of zinc doped tin oxide films prepared by spray pyrolysis technique *J. Phys. D. Appl. Phys.***41**
- [7] Kaviyarasu K, Manikandan E, Paulraj P, Mohamed S B and Kennedy J 2014 One dimensional well-aligned CdO nanocrystal by solvothermal method *J. Alloys Compd.***593** 67-70
- [8] Zhou Q, Mou Y, Ma X, Xue L and Yan Y 2014 Effect of fuel-to-oxidizer ratios on combustion mode and microstructure of Li₂TiO₃ nanoscale powders *J. Eur. Ceram. Soc.***34**
- [9] Rodney J D, Raja K, Deepapriya S, Vinosha P A, Mely L A, Priscilla S J, Daniel R and Das S J 2017 Investigation on the properties of Copper Oxide by Solution Combustion Synthesis *Int. Res. J. Eng. Technol.***04** 4-6
- [10] Priscilla S J, Daniel R, Gayathri S, Rodney J D, Thomas M, Ponraj C and Sivaji K 2017 Structural and Morphological properties of Lithium Doped Copper Oxide Nanoparticles *Int. J. Mater. Sci.***12** 245-9
- [11] Scherrer P 1918 Bestimmung der Größe und der inneren Struktur von Kolloidteilchen mittels Röntgenstrahlen *Math. Klasse***29** 98-100
- [12] Patterson A L 1939 The scherrer formula for X-ray particle size determination *Phys. Rev.***56** 978-82
- [13] Chang Y 1993 Fourier Transform Infrared (FTIR) Analysis of copper oxide thin films prepared by metal organic chemical vapour deposition (MOCVD) *Mater. Res. Soc. Symp. Proc.***293** 443
- [14] Piumetti M, Bensaid S, Andana T, Russo N, Pirone R and Fino D 2017 Cerium-copper oxides prepared by solution combustion synthesis for total oxidation reactions: From powder catalysts to structured reactors *Appl. Catal. B Environ.***205** 455-68
- [15] Lam, Pav, Mmj, Laj and S J Das 2017 Journal of Functional Materials and Biomolecules Investigations on the Effect of Reaction Time on SnS Nanostructures **1** 45-50
- [16] Jose M, Martin Britto Dhas S A, Daisy A D and Das S J 2016 Synthesis and characterization of nano spheres decorated silver bromide nanorods using a two step chemical reduction route *Opt. - Int. J. Light Electron Opt.***127** 8019-23
- [17] Li Y, Huang J, Cao L, Wu J and Fei J 2012 Optical properties of La₂CuO₄ and La_{2-x}CaxCuO₄ crystallites in UV-vis-NIR region synthesized by sol-gel process *Mater. Charact.***64** 36-42
- [18] Annie Vinosha P, Xavier B, Ashwini A, Ansel Mely L and Jerome Das S 2017 Tailoring the photo-Fenton activity of nickel ferrite nanoparticles synthesized by low-temperature coprecipitation technique *Optik (Stuttg.)***137** 244-53
- [19] Nair S S, Mathews M and Anantharaman M R 2005 Evidence for blueshift by weak exciton confinement and tuning of bandgap in superparamagnetic nanocomposites *Chem. Phys. Lett.***406** 398-403
- [20] Dar M A, Ahsanulhaq Q, Kim Y S, Sohn J M, Kim W B and Shin H S 2009 Versatile synthesis of rectangular shaped nanobat-like CuO nanostructures by hydrothermal method; structural properties and growth mechanism *Appl. Surf. Sci.***255** 6279-84
- [21] Wang W, Zhou Q, Fei X, He Y, Zhang P, Zhang G, Peng L and Xie W 2010 Synthesis of CuO nano- and micro-structures and their Raman spectroscopic studies *CrystEngComm***12** 2232.